Coacervation Is Promoted by Molecular Interactions between the PF2 Segment of Fibrillin-1 and the Domain 4 Region of Tropoelastin†

Adam W. Clarke,‡ Steven G. Wise,‡ Stuart A. Cain,§ Cay M. Kielty,§ and Anthony S. Weiss*,‡

School of Molecular and Microbial Biosciences G08, University of Sydney, Sydney, New South Wales, 2006, Australia, and Wellcome Trust Centre for Cell-Matrix Research, School of Biological Sciences, University of Manchester, Manchester M139PT, United Kingdom

Received March 23, 2005; Revised Manuscript Received May 2, 2005

ABSTRACT: In forming elastic fibers, microfibrils act as the scaffold sites for depositing the elastin precursor tropoelastin. We examined key binding interactions that promote massive tropoelastin association through coacervation. Using a segment of the microfibril protein fibrillin-1, PF2, known to bind full-length tropoelastin, we mapped its interaction site to the N-terminal region of tropoelastin bounded by domains 2 and 18. Precise contact residues between domain 4 of tropoelastin and domain 16 of fibrillin-1 were discovered through a novel combination of transglutaminase cross-linking and mass spectroscopy, with contact sites at residues K38 of tropoelastin and Q669 of fibrillin-1. This is the first report of a role for this region of tropoelastin in microfibril interactions. The addition of PF2 thermodynamically facilitated the coacervation of tropoelastin, resulting in smaller changes in entropy and enthalpy values for the coacervating system. A novel multicomponent *in vitro* tropoelastin assembly reaction system demonstrated that amassed tropoelastin was spatially and preferentially directed to surfaces coated with PF2 as expected for organized three-dimensional distribution during tissue elastogenesis. This study underscores the role of this part of fibrillin-1 as an anchor point for tropoelastin at the microfibril−elastin junction during the initial stages of elastic fiber assembly.

Elastic fibers are composed of elastin interspersed with microfibrils. These fibers play a crucial role in mediating elasticity in tissues such as artery, lung, and skin. The main component of microfibrils is fibrillin-1 (*1*). Fibrillin-1 is a large protein with multiple domains and is heavily glycosylated. It polymerizes in a head−tail fashion to form fibers that contain a beaded filament structure (*2*−*5*). The microfibrils form a scaffold onto which tropoelastin is deposited (*6*, *7*). Tropoelastin is the soluble precursor of elastin and consists of alternating hydrophobic and hydrophilic domains (*8*−*11*). It is one of a few proteins known to undergo a phase transition at physiological temperature. The process in which free tropoelastin monomers in solution assemble to form a cloudy mass is termed coacervation (*12*). This process is an important step in elastogenesis and is responsible for aligning and concentrating tropoelastin prior to cross-linking (*13*, *14*). Cross-linking occurs when the lysine side chains of tropoelastin are oxidized by lysyl oxidase (*15*). The irreversible process of cross-linking forms the end-product elastin, which is highly insoluble.

Of particular interest is the early interaction of tropoelastin with fibrillin-1. Along with acting as a molecular scaffold for tropoelastin deposition, it is proposed that fibrillin-1 aligns tropoelastin molecules prior to cross-linking (*6*). Because of the large and bulky nature of fibrillin-1, expressed fragments are studied for their ability to bind to tropoelastin. Recent studies indicate that multiple regions of fibrillin-1 are capable of binding tropoelastin with differing affinities. However, research has identified the fibrillin-1 fragment spanning exons 9−17 (PF2) as containing a major tropoelastin binding site (*16*, *17*). Further localization studies indicate that the binding site on this fragment of fibrillin-1 is in the eight-cysteine motif TB2. A model was proposed in which tropoelastin bound to this central region of fibrillin-1 identified as the shoulder interbead region of the fiber, prior to cross-linking (*17*).

In this study, we identified the region on tropoelastin to which PF2 binds and quantified the interaction between both binding partners on a multiregion basis. Using surface plasmon resonance (SPR),[1] we presented constructs of tropoelastin to PF2. We found that the N-terminal region of the tropoelastin region preferentially binds PF2. To further localize and independently verify the interaction site, we used a novel approach employing the cross-linking enzyme tissue

† A.W.C. and S.G.W. are recipients of an Australian Postgraduate Award. A.S.W. is a recipient of grants from the Australian Research Council and the University of Sydney Vice Chancellor's Development Fund.

* To whom correspondence should be addressed: School of Molecular and Microbial Biosciences G08, University of Sydney, Sydney, NSW, 2006, Australia. Telephone: +61-2-9351-3434. Fax: +61-2-9351-3467. E-mail: a.weiss@mmb.usyd.edu.au.

‡ University of Sydney.

§ University of Manchester.

[1] Abbreviations: cbEGF, calcium-binding epidermal growth factor; EDC, 1-ethyl-3-(3-dimethylaminopropyl)carbodiimide hydrochloride; EGF, epidermal growth factor; MAGP-1, microfibril associated glycoprotein-1; MS, mass spectroscopy; NHS, *N*-hydroxysuccinimide; LTBP-1, latent transforming growth factor−β-binding protein-1; Lys-C, endoproteinase from *Lysobacter enzymogenes*; SPR, surface plasmon resonance; TB domain, transforming growth factor−β-binding protein-like domain; Tgase, transglutaminase; tTgase, type-2 tissue transglutaminase; T_m of coacervation, temperature at the midpoint of coacervation; TMV, tobacco mosaic virus.

10.1021/bi050530d CCC: $30.25
Published on Web 07/09/2005

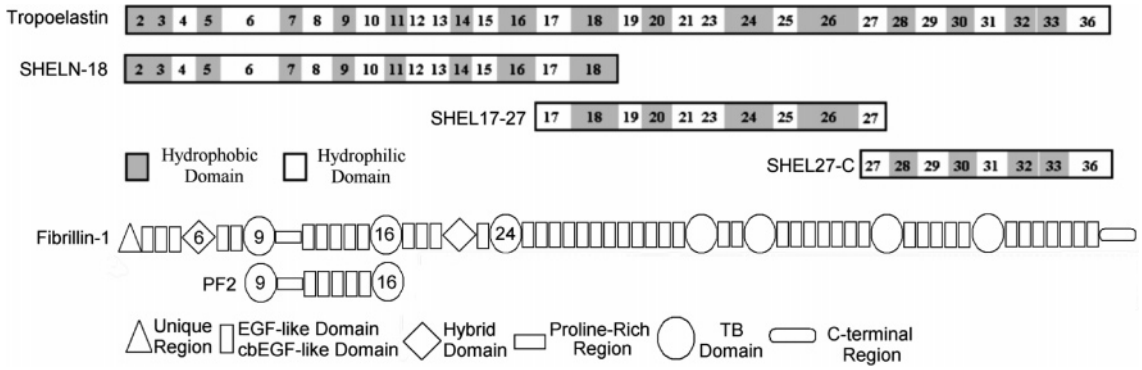

FIGURE 1: (a) Domain structure of human tropoelastin (SHELΔ26A). Constructs SHELN-18, SHEL17−27, and SHEL27−C collectively span the entire length of tropoelastin. Highlighted are the hydrophobic domains and lysyl oxidase cross-linking regions (hydrophilic domains). Numbers refer to tropoelastin domains. This diagram has been adapted from ref *40*. (b) Domain structure of fibrillin-1 with EGF domains, 8-cysteine unique region domain, hybrid domains, TB domains, the proline-rich domain, and the N-linked glycosylation sites shown. PF2 is shown for comparison. Numbers refer to specific domains of interest. This diagram was adapted from ref *17*.

transglutaminase (tTgase) and mass spectroscopy. Interacting contact regions were captured through a lysine−glutamine link, and the specific residues involved for both tropoelastin and fibrillin-1 were identified. Challenging the hypothesis that fibrillin-1 interacts late with pre-assembled tropoelastin during the coacervation stage of elastin assembly, we found that the change in entropy and enthalpy of coacervation was reduced in the presence of PF2. We also directly observed, using light microscopy, the formation of a coacervate around surfaces coated with PF2. This occurred at a large molecular excess of tropoelastin to PF2, indicating that, while coacervation primarily occurs through tropoelastin interactions, PF2 can mediate these interactions by binding to tropoelastin, thereby improving coacervation. The results support a model where this part of fibrillin-1 interacts with tropoelastin during the initial stages of elastic fiber assembly.

MATERIALS AND METHODS

Reagents. Full-length human tropoelastin (SHELΔ26A) lacking the region corresponding to exon 26A (*9*), SHELN-18 (*18*), SHEL17−27 (*19*), and SHEL27−C (*19*) was prepared as described previously. SHELN-18 spans the region of the SHELΔ26A gene corresponding to exons 2−18. SHEL17−27 spans the region corresponding to exons 17−27, while SHEL27−C spans the region corresponding to exon 27 to the C terminus (Figure 1A). All tropoelastin-related proteins were expressed recombinantly in *Escherichia coli* BL21(DE3). PF2 is a fibrillin-1 fragment that spans from exons 9−17 (residues 330−722) (Figure 1B). It was produced as previously described using a mammalian episomal expression system (*17*) and dialyzed into a HBS−Ca buffer (10 mM HEPES at pH 7.4, 0.15 M NaCl, 1 mM $CaCl_2$, and 0.005% surfactant P20) in preparation for Biacore analysis. The purity of each construct was examined using SDS−PAGE (*20*), and the concentration was determined using the BCA protein assay (Pierce).

Sequence numbers given for tropoelastin correspond to GenBank entry AAC98394 (gi 182020) from amino acid 27−724 and describe the mature protein following the removal of the signal peptide. Fibrillin-1 fragment PF2, encoded by exons 9−17, corresponds to residues 330−722 of GenBank entry AB177803 (gi 46559357) and contains a 6× His N-terminal tag. Endoproteinase Lys-C was purchased from Calbiochem. tTgase from guinea pig liver was obtained from Sigma. All other reagents were of analytical grade.

SPR Analysis of Molecular Interactions. Kinetic analysis of the binding between PF2 and tropoelastin was examined using SPR. The Biacore 3000 system was used for this study (Biacore AB, Sweden). Tropoelastin, SHELN-18, SHEL17−27, and SHEL27−C were immobilized onto the surface of a CM5 research-grade sensor chip using amine coupling. This was performed using 1-ethyl-3-(3-dimethylaminopropyl)-carbodiimide hydrochloride (EDC), followed by *N*-hydroxysuccinimide (NHS) and ethanolamine-HCl, as described by the manufacturer. All proteins were dissolved in sodium acetate at pH 3.0 and then immobilized on the chip at a flow rate of 30 μL/min in HBS−Ca buffer. This gave the following response levels: tropoelastin, 1665 RU (response units); SHELN-18, 3247 RU; SHEL17−27, 4179 RU; and SHEL27−C, 2585 RU. On a single flow cell, the dextran matrix was treated as described above but without the protein present to provide a blank flow cell for these studies. All sensorgram data presented were subtracted from the corresponding data from the blank cell.

PF2-Binding Full-Length Tropoelastin Using SPR. Sensorgrams were obtained for PF2 binding to the immobilized tropoelastin using HBS−Ca buffer. PF2 at various concentrations (5.1−0.3 μM) were prepared by dilution in HBS−Ca. These concentrations were injected for 3 min at a flow rate of 60 μL/min with a sampling rate of 5 Hz. Regeneration was performed after 15 min of dissociation using 1 M NaCl and 10 mM glycine for 2 min. A typical experiment used the five PF2 concentrations and a control containing no PF2, followed by a regeneration step that was measured successful when the baseline returned to zero.

Rate constants for association (k_a) and dissociation (k_d) and the equilibrium dissociation constant (K_D) were obtained by globally fitting the data using the BIAevaluation software version 3.0 using the simple 1:1 Langmuir binding model. This method was preferred because the equilibrium binding state was not reached. All experiments were duplicated. Statistical analysis of the curve fitting at both dissociation and association phases of the sensorgrams showed low χ^2 values (<2).

PF2-Binding Tropoelastin Constructs Using SPR. Sensorgrams were obtained for PF2 binding to the immobilized

constructs using HBS−Ca buffer. PF2 at various concentrations (4.1−0.3 μM) for immobilized SHELN-18 and (2.3−0.14 μM) for immobilized SHEL17−27 and SHEL27−C were prepared by dilution in HBS−Ca along with a control containing no PF2. They were then injected for 3 min at a flow rate of 60 μL/min with a sampling rate of 5 Hz. Regeneration was performed after 15 min of dissociation using 1 M NaCl and 10 mM glycine for 2 min. All experiments were repeated in duplicate. Data analysis was performed as described above.

In Vitro Cross-Linking of PF2 with Tropoelastin Using tTgase. tTgase from guinea pig liver was used to cross-link tropoelastin with PF2. The reaction protocol was adapted from ref *17*. Tropoelastin (100 μg) was reacted with PF2 (100 μg) in the presence of tTgase (10 μg) in 100 μL of reaction buffer (0.174 M Tris-hydroxymethyl-methylamine, 8.7 mM reduced glutathione, and 4 mM $CaCl_2$) by incubation overnight at 25 °C. Cross-linking was analyzed using SDS−PAGE and Western blots as previously described (*17*).

Mass Spectrometry. Endoproteinase Lys-C (Lys-C) digestion of cross-linked proteins was carried out in 500 μL of milli-Q water using 1 mg of protein, incubated at 25 °C overnight at an enzyme−substrate ratio of 1:1000. Samples were subsequently diluted to reach a target concentration of 20 μg per 100 μL in 1% formic acid. A water/acetonitrile gradient was run over 25 min at a flow rate of 200 nL/min, until acetonitrile was 60% of the eluent. Experiments were carried out on a Q-Star Pulsar API nano LC−MS/MS (Applied Biosystems, with the assistance of Mark Raftery, Biomedical Mass Spectroscopy Facility, University of New South Wales, Australia).

Software Assignments. Raw masses from the Q-Star were assigned as cross-linked species using the Automated Spectrum Assignment Program (*21*). For the human tropoelastin sequence, the mass change upon cross-linking was set at −17 Da for tTgase cross-linking (Figure 3). Up to three missed cleavages were allowed, and error tolerances were set at 0.10 Da. The specificity of Lys-C was assumed to be exclusive for lysine residues. No amino acid modifications were permitted. MS/MS spectra were interpreted using MS2Assign (*22*). Peptide sequences and cross-linking positions were defined, while the mass change on cross-linking and lack of amino acid modification remained unchanged. All possible fragmentation ions were included in the data analysis (a, b, c, x, y, z). Error tolerances of 0.05 Da were set for MS/MS confirmations.

Coacervation of Tropoelastin with PF2. Tropoelastin was prepared in phosphate-buffered saline (PBS) at a concentration of 78 μM. PF2 was prepared in sterile water at a concentration of 3 μM. BSA was prepared in sterile water at a concentration of 3 μM. Titration reactions containing tropoelastin (62 μM) were mixed with PF2 or BSA giving final concentrations of 0, 150, 300, 450, and 600 nM. Each reaction mixture was transferred to a quartz cuvette (500 μL capacity) for light-scattering measurements at 300 nm. A Shimadzu UV-1601 UV−vis spectrophotometer, fitted with a heating/cooling block, was regulated by a circulating water bath capable of heating and cooling the water. This allowed light scattering to be measured under different temperature conditions. A typical coacervation reaction began by cooling the block to 15 °C. The reaction mixtures where then placed into the block and blanked with an equivalent PBS water mixture. The temperature of the system was set to 60 °C, and a time course of OD was measured as the temperature of the system rose. The temperature rise was also measured using a thermometer proportionate to the time course. A trendline of the temperature−time relationship was constructed, and the slope and intercept of the trendline were used to interconvert between the two values. A plot was then generated of OD versus temperature. The midpoint between the baseline and the maximum OD of coacervation was calculated using curve-fitting software (GraphPad Prism 4.0) and reported as the temperature at the midpoint of coacervation (T_m of coacervation). The time taken to reach the midpoint of coacervation for various concentrations of tropoelastin (0.1−5.0 mg/mL) with and without PF2 (1−600 nM) was also measured. This was performed by fixing the water bath to a constant temperature of 40 °C. All solutions were cooled on ice and then placed in the spectrophotometer, and the OD as a function of time was measured. The midpoint of coacervation was determined from these plots, and the time corresponding to the midpoint of coacervation was determined. A plot of time (in seconds) versus the concentration of tropoelastin was generated. All curves and trendlines were fitted with an R^2 value of at least 0.99. The reversibility of the system was demonstrated by rapidly heating the system to 50 °C until coacervation occurred and then cooling the system to 15 °C.

Solution Thermodynamic Calculations of Coacervation of Tropoelastin in the presence of PF2. The effect of adding PF2 to a high concentration (262 μM) and low concentration (72 μM) of tropoelastin was measured by thermodynamic calculations. Tropoelastin solutions containing 600 nM BSA or 80 nM PF2 were heated to various temperatures between 15 and 37 °C, and the OD at maximum coacervation was measured at 300 nm. These data were plotted, and the data points that lie on the transitional phase of the curve were used to produce a van't Hoff plot, according to the method of Lauffer (*23*). Using the relationship that turbidity (τ) = 2.303(OD), the change in enthalpy (ΔH) and entropy (ΔS) was estimated using the relation

$$\log e(\tau^2 - \tau_o^2) - \log e(\tau_m - \tau)^2 = \log[2\tau_o + 2.303(\mathrm{OD} - \mathrm{OD_o})] + \log[2.303(\mathrm{OD} - \mathrm{OD_o})]\ 2\log[2.303(\mathrm{OD_m} - \mathrm{OD})] = \left(\frac{\Delta S}{2.303R} + \log(4m\tau_o^2) - 2\log[\tau_o + 2.303(\mathrm{OD_m} - \mathrm{OD_o})]\right) - \frac{\Delta H}{2.303RT} \quad (1)$$

where OD is the maximum turbidity of the coacervate at a given absolute temperature (T), OD_o is the minimum turbidity, OD_m is the maximum turbidity of the coacervate at a given concentration of tropoelastin, R is the molar gas constant, and m is the molar protein concentration of the solution. The value of the constant τ_o was assumed to be 0.002 (*24*). From the above equation, a linear plot was generated of which the slope equals $-(\Delta H/2.303R)$ and the y-axis intercept

$$\frac{\Delta S}{2.303R} + \log(4m\tau_o^2) - 2\log[\tau_o + 2.303(\mathrm{OD_m} - \mathrm{OD_o})] \quad (2)$$

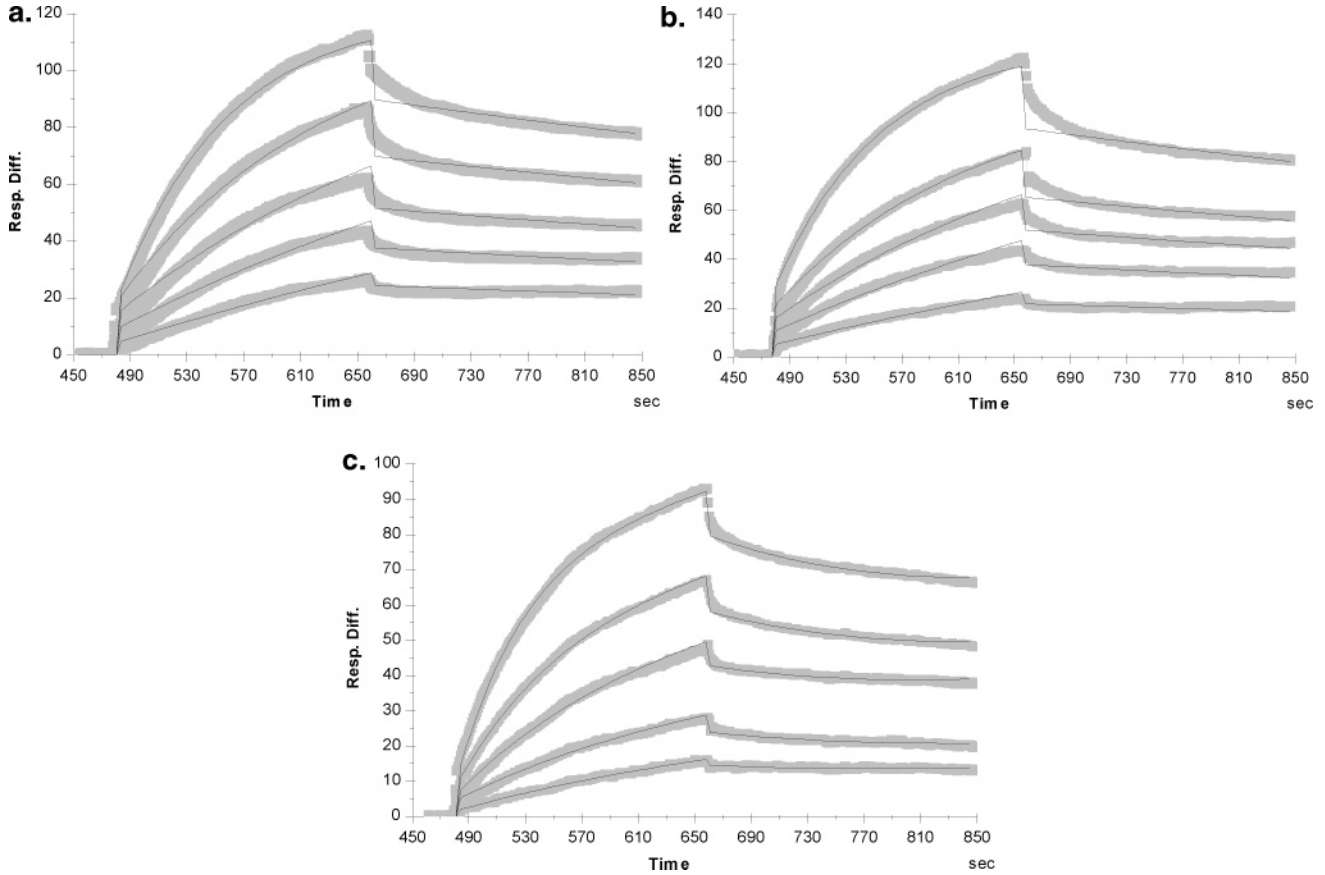

FIGURE 2: Interaction of PF2 with tropoelastin constructs using SPR. Fibrillin-1 fragment PF2 was injected over tropoelastin (a), SHELN-18 (b), SHEL17-27 (c), and SHEL27C (data not shown) immobilized sensor chips. Each sensorgram shows the average result of five different concentrations (duplicates) of PF2 (gray traces). Each sensorgram was subtracted from the response of a blank cell, along with the response from the buffer alone. A fit of the sensorgrams was obtained using BiaEvaluation 3.0.2 software and the Langmuir 1:1 binding isotherm (solid black line). Response difference refers to the difference between experimental and blank cells in response units (RU). Time is in seconds.

The Gibbs free energy was calculated at 37 °C using the equation $\Delta G = \Delta H - T\Delta S$.

Tropoelastin Coacervation around a PF2-Coated Surface. Ni−NTA agar beads (Qiagen) were incubated with a solution of PF2 (5 mg/mL). Binding was confirmed by using Western blot. A sufficient tropoelastin solution (10 mg/mL) was used to cover the well bottom of a 96-well microtiter plate. Using an inverted light microscope (Olympus), coacervation was observed as the solution was gently heated to 40 °C. In a separate well, coacervation was then observed in the presence of a small number of uncoated agar beads to serve as a control. PF2-coated beads were then added separately; coacervation was reached, followed by cooling; and the solution was heated again. The coacervate was then allowed to remain at 40 °C for 30 min during which time the coacervate in solution settled to the bottom of the well. Photographs were taken using a mounted Olympus camera.

RESULTS

Binding of PF2 to Tropoelastin Constructs Using SPR. Tropoelastin and PF2 were found to be pure as determined by SDS−PAGE. The interaction of PF2 with tropoelastin, SHELN-18, SHEL17−27, and SHEL27C was investigated using SPR. Strong PF2 binding was observed in the presence of calcium for full-length tropoelastin, with an equilibrium dissociation constant (K_D) of 322 ± 12 nM (Figure 2a and Table 1). This result compares well to the published K_D of 279 ± 125 nM (*17*). The construct SHELN-18 encompassing domains 2−18 of full-length tropoelastin bound PF2 tightly with a K_D of 270 ± 8 nM (Figure 2b and Table 1) stronger than that of full-length tropoelastin. SHEL17−27 bound PF2 with a K_D of 577 ± 22 nM (Figure 2c and Table 1). PF2 did not quantitatively interact with SHEL27−C.

Table 1: Kinetic Data for Analysis of PF2 Binding to Tropoelastin Constructs Using SPR[a]

construct analyte	k_a (1/Ms)	k_d (1/s)	K_D (nM)	χ^2
tropoelastin	$2.41 \pm 0.05 \times 10^3$	$7.74 \pm 0.13 \times 10^{-4}$	322 ± 12	1.4
SHELN-18	$3.04 \pm 0.04 \times 10^3$	$8.20 \pm 0.15 \times 10^{-4}$	270 ± 8	1.2
SHEL17-27	$7.52 \pm 0.07 \times 10^3$	$4.34 \pm 0.12 \times 10^{-3}$	577 ± 22	0.2

[a] Kinetic analysis of the binding of PF2 to tropoelastin constructs. Values are the mean determination from five different concentrations run in duplicate. The standard error (SE) is also given. k_a refers to the rate association constant; k_d refers to the rate dissociation constant; and K_D refers to the equilibrium dissociation constant. χ^2 is a measure of the goodness of the fit (typically <2 is a good fit).

Further Identification of the Contact Site of Tropoelastin with PF2. tTgase forms cross-link(s) between tropoelastin monomers and the fibrillin-1 fragment PF2 (*17*). Typical total reaction samples containing tropoelastin and tTgase, PF2 and tTgase, and tropoelastin, PF2, and tTgase were digested with Lys-C. From mass spectra, tTgase-derived cross-links were observed as homotypic with tropoelastin and PF2 and heterotypic as a tropoelastin-PF2 cross-link. The specific

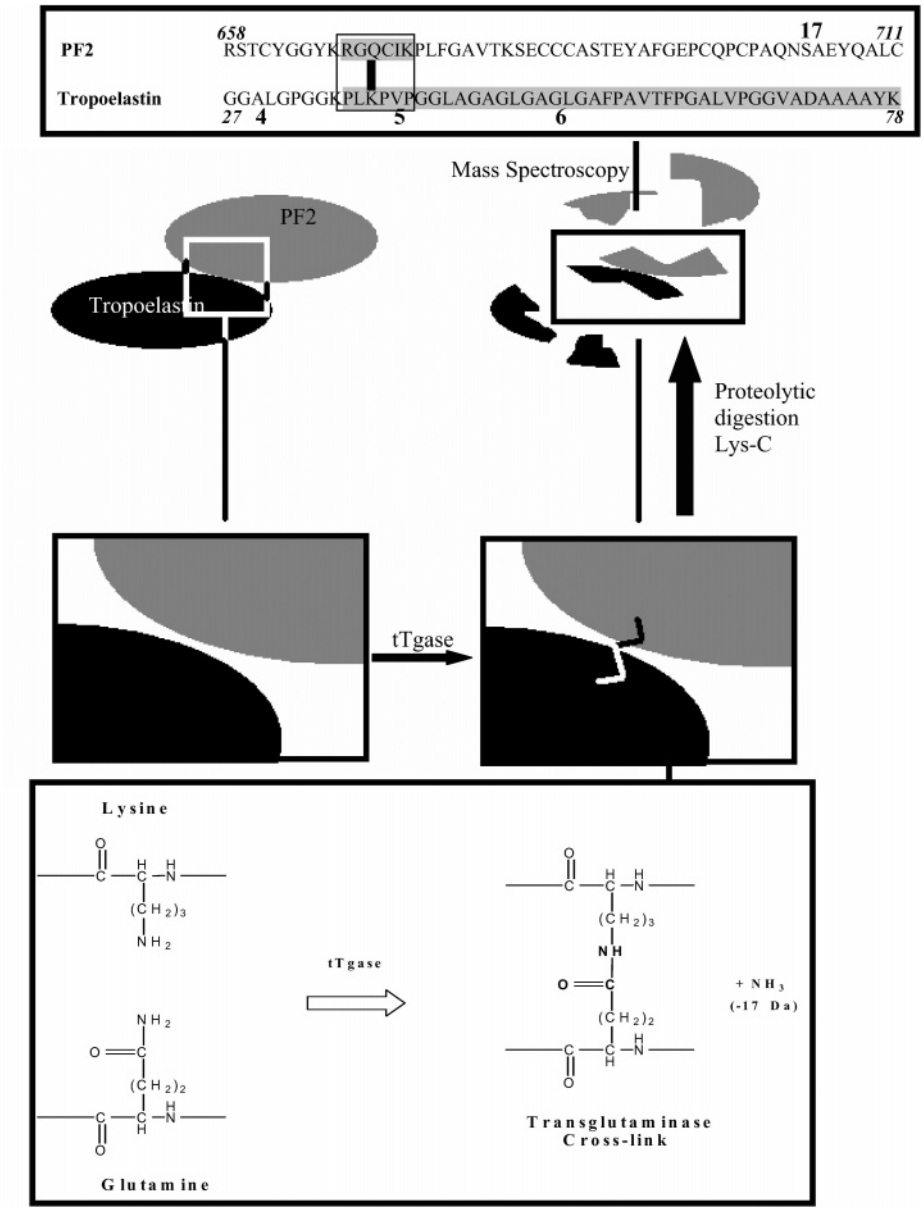

FIGURE 3: Experimental method used in this study and the resulting PF2−tropoelastin cross-link. Tropoelastin and PF2 were incubated in the presence of tTgase, which mediates a cross-link between a glutamine and a lysine residue. The resulting cross-linked mixture was then digested with Lys-C, and mass spectroscopy was performed on the resulting fragments to identify a tropoelastin−PF2 cross-link.

cross-linked species corresponded to residues 36−K38−78 of tropoelastin and 667−Q669−672 of fibrillin-1 (Figure 3), linking residues K38 and Q669, respectively.

Further confirmation of this cross-link was obtained using tandem mass spectrometry data (MS/MS) gathered in series. In all, 17 masses from MS/MS spectra were assigned to peptide fragments from the intact link identified using ASAP (Table 2). After the common losses of carbon monoxide, water, and ammonia were accounted for, 100% sequence coverage was obtained.

Coacervation Titration of PF2 with Tropoelastin. Increasing PF2 was titrated with tropoelastin, and the time course of coacervation properties was measured. As the concentration of PF2 increased, the T_m of coacervation decreased (Figure 4a). At a concentration of 600 nM PF2, the T_m of coacervation was 7.2 °C lower than tropoelastin with BSA. This was not due to a nonspecific nucleating effect as was demonstrated by replacing PF2 with BSA. The time taken to reach midpoint of coacervation was slightly quicker when adding PF2 to tropoelastin especially at tropoelastin concentrations below 1 mg/mL (Figure 4b). Because coacervation is a temperature-dependent reversible process, the effect of PF2 on the reversibility of coacervation of tropoelastin was also measured (*12*). Tropoelastin with 600 nM PF2 was heated repeatedly to 50 °C and cooled to 15 °C, verifying the reversible nature of the system (Figure 4c).

Solution Thermodynamics of Tropoelastin Coacervation in the Presence of PF2. The OD of maximal coacervation of tropoelastin changed with respect to the temperature and concentration of tropoelastin (Figure 5a). van't Hoff plots for different concentrations of tropoelastin were produced (parts b and c of Figure 5). The effect of adding PF2 to these systems was measured in comparison to BSA. Using the method of Lauffer (*23*), the enthalpy and entropy changes and Gibbs energy were calculated from these plots (Table 3). In the presence of BSA and PF2, coacervation of tropoelastin is an endothermic, entropy-driven process confirming previous studies (*12*). The enthalpy and entropy

Table 2: MS/MS Fragment Mass Assignments of Tropoelastin−PF2 Cross-Link[a]

MHobs	ion	sequence tag	error
1226.6958	FPAVTFPGALVPG-28	FPAVTFPGALVPG	0
1151.6851	a-int(b)-18	FPAVTFPGALVP	0.02
1123.7328	[b(a)y(b)/b(b)y(a)]+ +18	QCIK−PLKPVP	0.05
708.3544	GAGLGAGLGA-17	GAGLGAGLGA	−0.01
698.3968	a-int(b)-18	GLGAGLGAF	0
637.3333	GGLAGAGLG-17	GGLAGAGLG	0
609.3239	GVADAAAA-18	GVADAAAA	0.02
580.3392	GLGAGLGA-17	GLGAGLGA	0.03
481.2612	VADAAA-18	VADAAA	0.02
453.2322	PGGLAG	PGGLAG	−0.01
342.2103	c-int(b)	PGGL	0
325.1632	GVAD-18	GVAD	0.01
268.1881	a-int(b)-17	LAGA	0.02
172.1151	AGA-28	AGA	0.01
155.0794	PG	PG	0
86.0867	I(a) imm	I	−0.01
72.0779	V(b) imm	V	0

[a] Masses (Da) from Q-Star analyses (bottom) matched with the peptide fragments of the sequence from the cross-link pair: RGQCIK, PLKPVPGGLAGAGLGAGLGAFPAVTFPGALVPGGVADAAA-AYK.

changes and Gibbs free energy changed substantially at lower concentrations of tropoelastin. The changes in enthalpy and entropy of coacervation were significantly smaller in the presence of PF2 at high concentrations of tropoelastin.

Tropoelastin Coacervates around a PF2-Coated Surface. The process of tropoelastin coacervation was observed under an inverted light microscope and appeared as the formation of droplets (Figure 6) that grew over time. This was consistent with previous findings using α elastin (*25*). When uncoated agarose beads were placed in a solution of tropoelastin and heated, coacervation occurred in solution but no significant interaction of the coacervate with the bead was observed (Figure 7). In contrast, when PF2-coated beads were placed in a tropoelastin solution, coacervation occurred in solution, around the beads, and also on the surface of the beads. When the temperature was lowered, the reversibility of the system was demonstrated and the coacervate dissipated from the bead surface (Figure 8). When heat was again applied, the coacervate occurred on the surface of the beads and in solution (Figure 9). After a period of time, the coacervate in solution settled, while the beads retained coacervate droplets (Figure 9E).

DISCUSSION

Because of the large size of fibrillin-1, it has been necessary to explore individual specific regions of the protein. A region near the N terminus of fibrillin-1, encompassed by the fragment PF2, is on the shoulder of the interbead region and has been identified as a major site of tropoelastin deposition (*16*, *17*, *26*). To date, previous studies, using

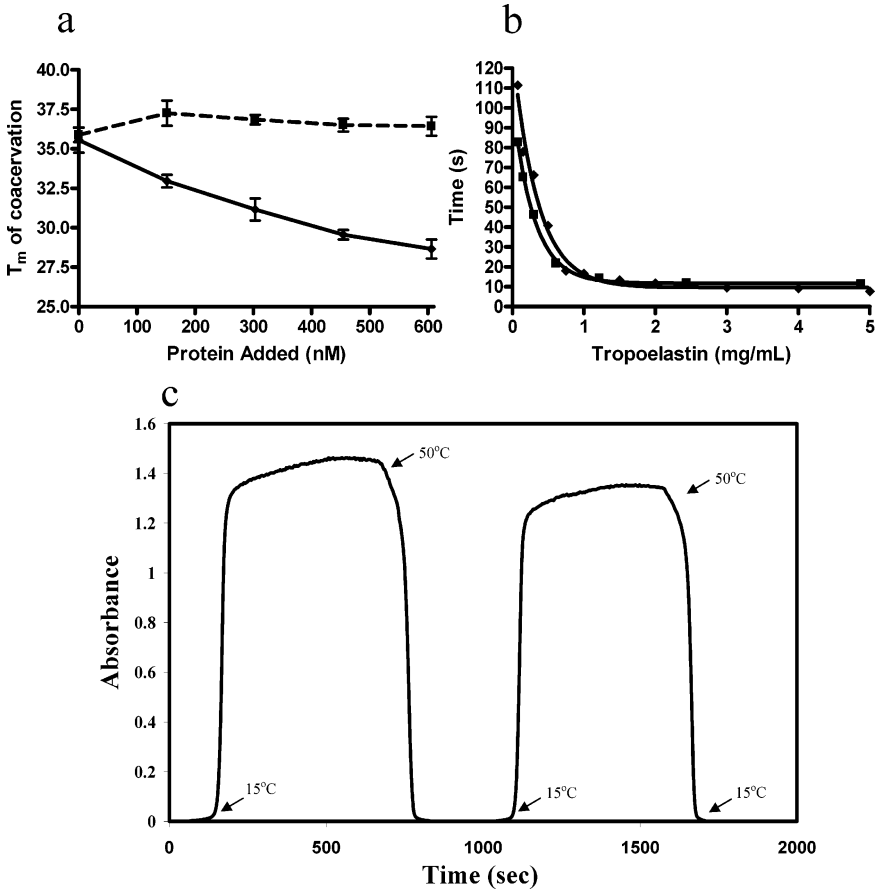

FIGURE 4: (a) Temperature at the midpoint of coacervation (T_m of coacervation) was measured. The T_m of coacervation decreased upon adding increasing amounts of PF2 (—). The addition of BSA showed a small increase in the T_m of coacervation (···). (b) Tropoelastin at different concentrations (0.1−5 mg/mL) was coacervated at 40 °C, and the time taken to reach midpoint of coacervation was measured (◆). This process was repeated with PF2 added (1.2−600 nM) to concentrations of tropoelastin (0.1−4.8 mg/mL) (■). (c) True coacervation requires that the process is reversible. PF2 was added to tropoelastin, and the solution was rapidly heated and cooled, showing the reversibility of the system.

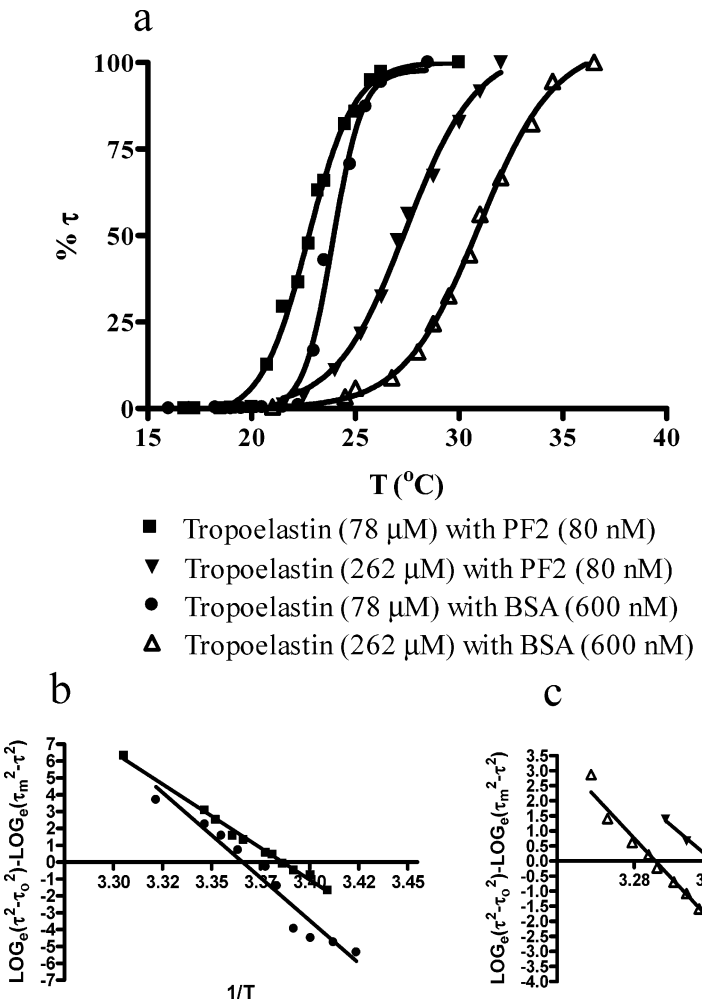

FIGURE 5: Thermodynamic properties of the coacervation of tropoelastin in the presence of PF2. (a) A low concentration tropoelastin solution (78 uM) was mixed with 600 nM BSA. The resulting maximum OD of coacervation was measured and converted into % turbidity at specific temperatures (●). This process was repeated using a high concentration of tropoelastin (262 uM) (△). The experiment was repeated with the same low concentration (■) and high concentration (▼) stock of tropoelastin however PF2 (80 nM) was added. (b) Turbidity data derived from (a) was plotted against the inverse of temperature according to the method of Lauffer (*23*). The slope and intercept on the *y* axis when $1/T = 0$ was used to estimate the ΔH and ΔS for coacervation of tropoelastin at low concentration (●) and with added PF2 (80 nM) (■). (c) Turbidity data derived from (a) were used to estimate the ΔH and ΔS, for the coacervation of a high concentration of tropoelastin (△) and in the presence of PF2 (80 nM) (▼).

Table 3: Thermodynamic Properties of Coacervation in the Presence of PF2[a]

solution	ΔH (kJ mol^{-1})	% ΔH	ΔS (J mol^{-1} K^{-1})	% ΔS	ΔG (kJ mol^{-1})	% ΔG
tropoelastin (72 μM) + BSA (600 nM)	1943 ± 162	74 ± 6	6719 ± 564	75 ± 6	−171 ± 28	75 ± 12
tropoelastin (72 μM) + PF2 (80 nM)	1448 ± 41		5087 ± 143		−129 ± 7	
tropoelastin (262 μM) + BSA (600 nM)	1049 ± 53	82 ± 4	3634 ± 185	84 ± 3	−78 ± 8	107 ± 11
tropoelastin (262 μM) + PF2 (80 nM)	856 ± 19		3031 ± 68		−84 ± 3	

[a] Measurements for the enthalpy (ΔH) and entropy (ΔS) and Gibbs free energy (ΔG) of the system are given during the process of coacervation according to the method of ref *23*. The percentage values with standard error are the differences between the enthalpy and entropy and Gibbs free energy of coacervation in the presence of PF2 compared to these values in the presence of BSA.

methods such as exon deletion, have suggested that C-terminus regions of tropoelastin are involved in elastin deposition on microfibrils (*27*). In this study, we demonstrate for the first time that the PF2 region of fibrillin-1 binds multiple sites in full-length tropoelastin. We present SPR evidence that PF2 binds strongly to the N-terminal region of tropoelastin, encompassing domains 2−18 with a dissociation constant lower than that of the full-length protein. An additional weaker PF2-binding site was identified in domains 17−27. With the possibility of multiple regions of tropoelastin forming the major binding site for PF2, a more localized binding site was sought along with additional confirmation of this interacting region.

Recent advances in mass spectrometry have enabled the rapid analysis of complicated digested cross-link proteins. As such, the use of cross-linking probes to identify protein folds and interactions has become far more common (*21*). We sought to verify the interaction between PF2 and tropoelastin, using tTgase as a cross-linking probe to trap the contact point between these two proteins. tTgase was chosen for its ability to cross-link glutamine and lysine residues of which tropoelastin and PF2 contain an abundance.

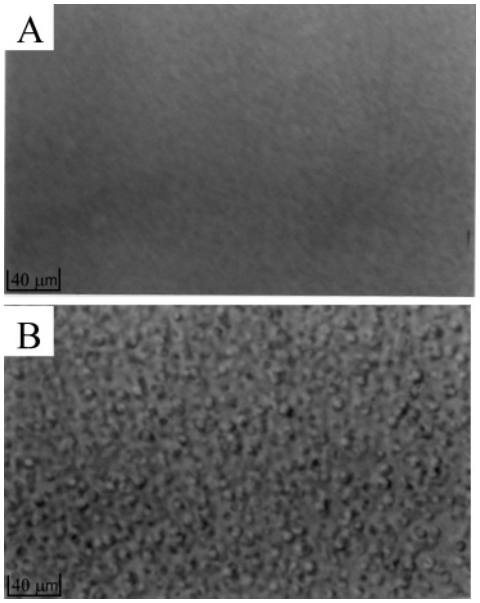

FIGURE 6: Tropoelastin coacervation in solution. As viewed through an inverted light microscope, tropoelastin in solution was clear at 15 °C (A). As heat was applied a tropoelastin coacervate formed as visible droplets of increasing size, as viewed at 40 °C (B).

These amino acids are evenly distributed throughout both proteins, making tTgase an excellent cross-linking reporter enzyme. Of a possible 613 (35 lysines on tropoelastin with 15 glutamines on PF2 or 8 glutamines on tropoelastin with 11 lysines on PF2) cross-links that could have formed, a single cross-link was observed. In support of the strong binding observed for the SHELN-18 construct of tropoelastin, a cross-link was identified at lysine 38 in domain 4 of tropoelastin. On fibrillin-1, we identified glutamine 669 (Q699) as the involved residue. tTgase cross-links proteins if their participating residues are spatially very close, and tTgase is not sterically hindered by surrounding residues. We interpret this to mean that the residues involved at the identified contact point of PF2 with tropoelastin come into very close proximity, suggesting that the major PF2 binding site is located within this domain of tropoelastin. The binding of PF2 to domains 17−27 was also observed; however, no cross-links were captured in this region, indicating that this interaction site was inaccessible for tTgase cross-linking.

Further examination of the contact site on tropoelastin identifies two lysines in close spatial arrangement, confirming suggestions in previous studies that the interaction is mediated by exposed lysines of tropoelastin (*16*). Structural studies on human tropoelastin have been limited to date, making conformational analysis of this region of tropoelastin difficult (*28*). Previous studies on the tropoelastin-binding site on PF2 drew specific attention to the TB2 region, encoding domains 16 and 17 (*17*). The identified cross-link at Q669 is within this region at domain 16. Further, recent mass spectra data suggest that Q669 is exposed on tissue microfibrils from nonelastic ciliary zonules and available to be cross-linked

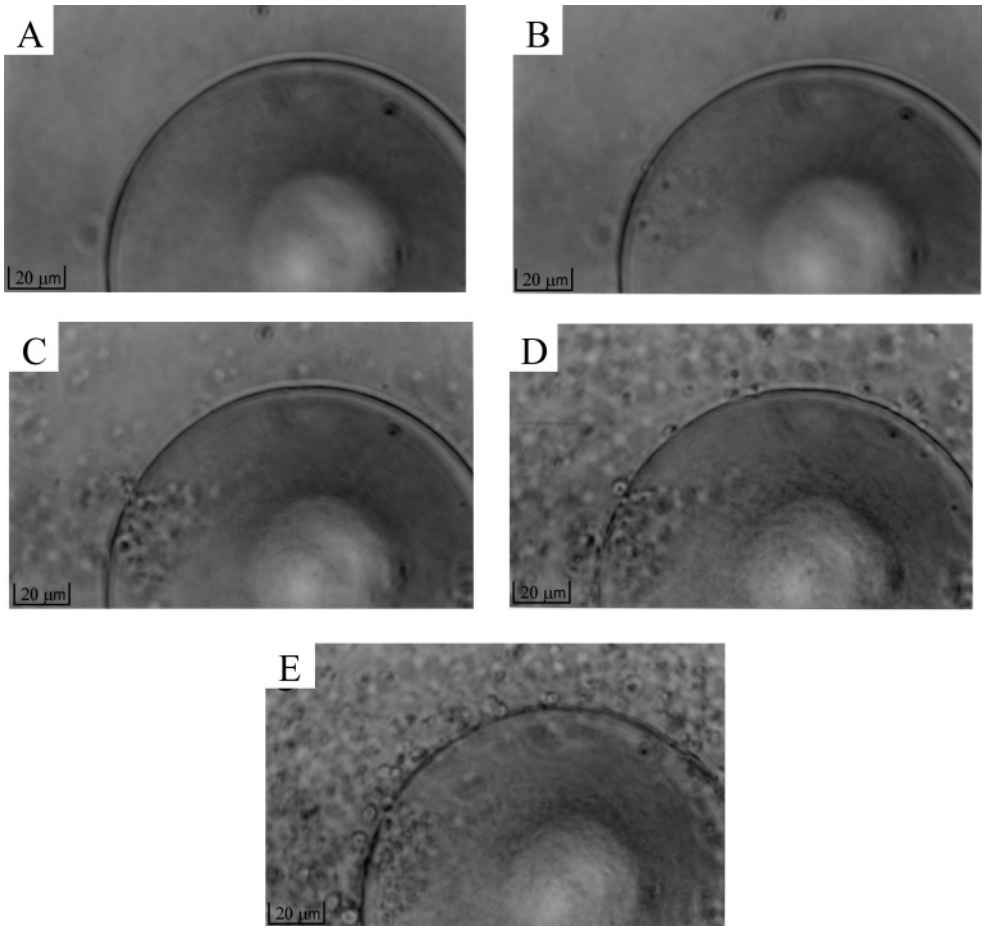

FIGURE 7: Tropoelastin does not interact specifically with control uncoated agar beads. Uncoated Ni−NTA agar beads were placed in a tropoelastin solution which was allowed to equilibrate on ice. It was then incubated at 40 °C and coacervate formation was photographed at (A) 60 s, (B) 65 s, (C) 70 s, (D) 75 s and (E) 80 s after incubation.

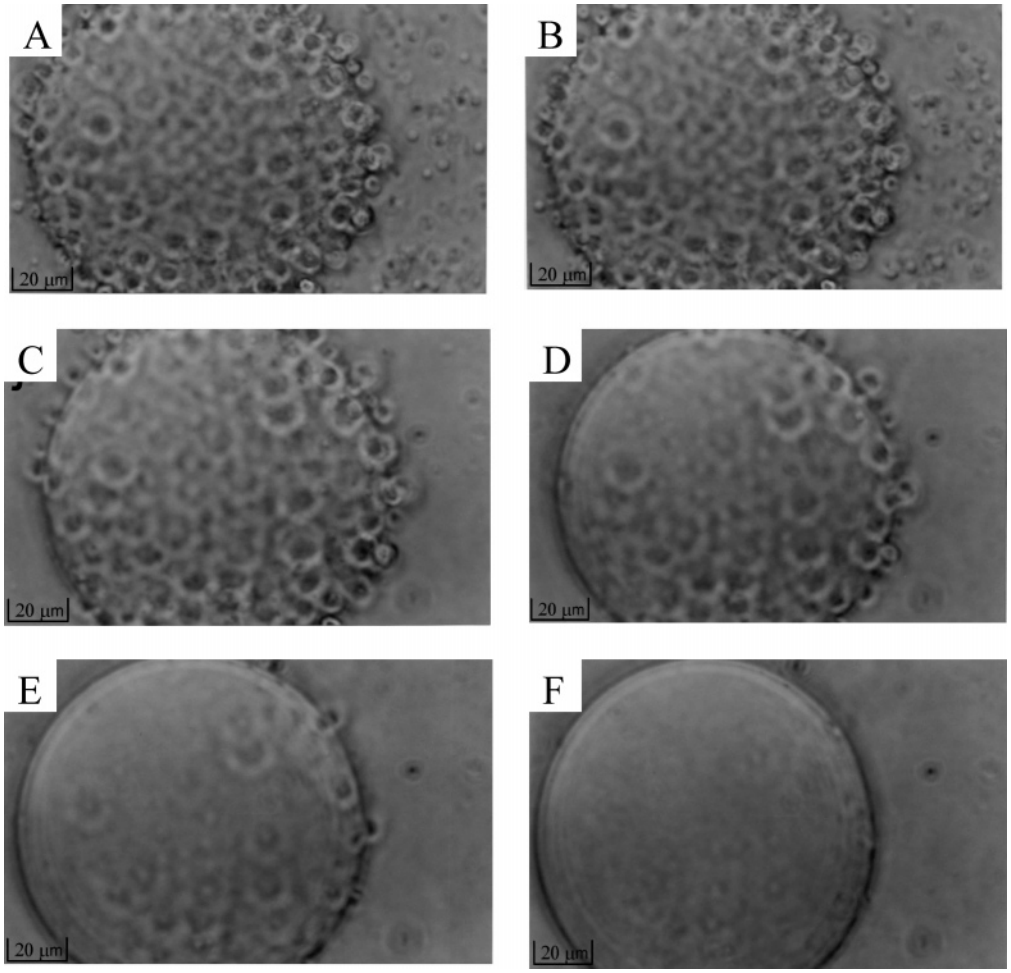

FIGURE 8: Coacervating tropoelastin interacts with PF2 coated agar beads and dissipates upon cooling. PF2 was incubated with Ni−NTA agar beads and binding to the beads via the 6XHis tag of PF2 was confirmed using western blots (not shown). The coated beads were then placed in a tropoelastin solution which was incubated at 40 °C and then rapidly cooled. The images were photographed at (A) 80 s, (B) 90 s, (C) 100 sec, (D) 120 s, (E) 140 s and (F) 160 s after cooling.

with protein partners (Cain, S. et al., manuscript in preparation).

While our *in vitro* finding sheds new light on the nature of the fibrillin-1 tropoelastin interaction, we sought further physiological evidence of their interaction during the coacervation stage of elastogenesis. The most widely accepted model of coacervation attributes the process to the disruption of ordered water around the hydrophobic regions of the tropoelastin monomer, exposing them and allowing these regions to interact in a tight hydrophobic manner (*12*, *14*). Recent studies have identified domains 19−25 of tropoelastin as being interaction sites during coacervation (*29*). Multiple hydrophobic interactions between tropoelastin monomers occur, forming a coacervate.

Tropoelastin coacervation is a reversible process. Previous studies have shown it to be endothermic, entropy-driven (*12*). Of interest are previous studies that identified molecules, such as heparin, chondroitin sulfate B, and 1,1,1-trifluoroethanol, that could influence tropoelastin coacervation (*30*, *31*). However, unlike these previous molecules, PF2 addition supported the reversible nature of the system. The coacervation of tropoelastin was monitored as increasing amounts of PF2 were titrated into the system and showed a shift to a lower T_m of coacervation compared to tropoelastin only in solution. This result is likely to explain the subsequent discovery that tropoelastin solutions containing PF2 reach their midpoint of coacervation more quickly than those lacking PF2. Because a lower temperature is required to coacervate a tropoelastin solution containing PF2, when a solution is heated to 40 °C, it would reach its midpoint of coacervation faster than a normal tropoelastin solution. This process was due to thermodynamic effects. The thermodynamic properties measured in this study are higher than in previous studies (*12*). This is due to the different concentrations used in this study. Our thermodynamic values compare well to those of collagen type I (*32*) and tobacco mosaic virus (TMV) (*23*). This study is modeled on that of TMV, which undergoes a similar phase-transition polymerization. The mechanism of polymerization can be approximated using the mathematics of linear condensation polymerization. This model is relevant in examining the coacervation of tropoelastin, because it has been shown that different regions of the tropoelastin monomer can be involved in hydrophobic interactions at any given time (*29*). Direct light-scattering measurements have long been the method for determining the thermodynamic properties of solutions that undergo these phase transitions (*23*, *24*, *38*, *39*).

From these thermodynamic studies, the changes in enthalpy and entropy of the coacervating system were smaller in the presence of PF2. The T_m of coacervation was lower in the presence of PF2. This can be explained by its correspondingly smaller change in the enthalpy value.

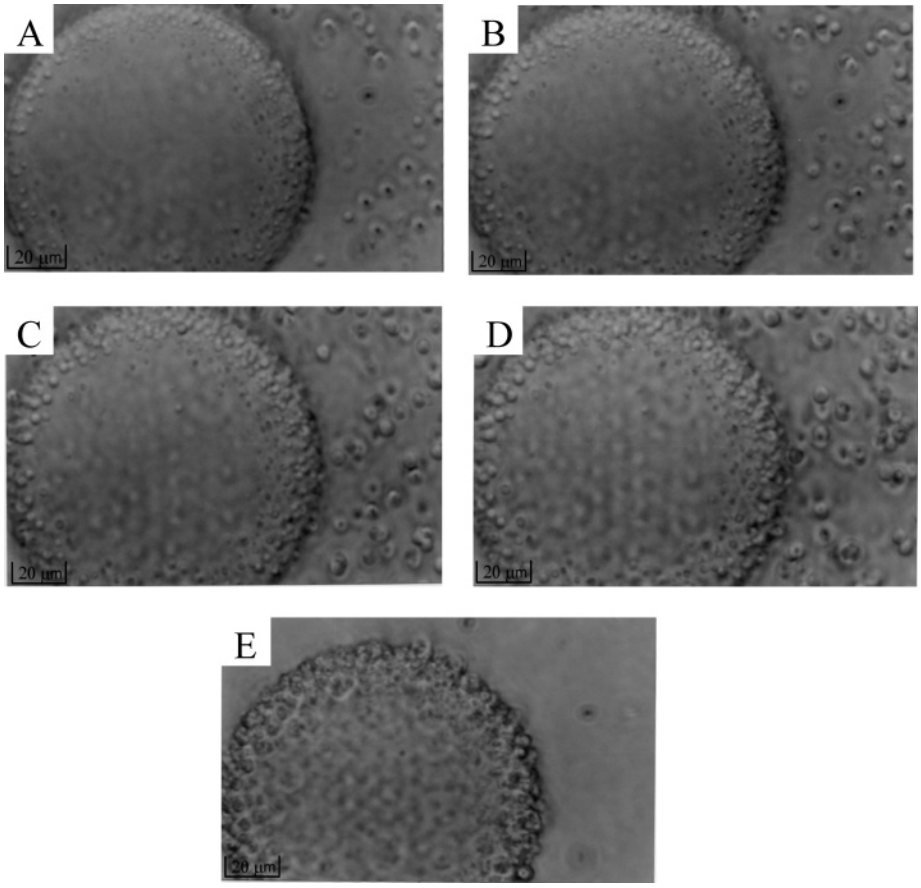

FIGURE 9: Coacervate droplets of tropoelastin reversibly interact with PF2 coated agar beads. After a coacervate was formed on the coated bead surface and dissipated by cooling, the same tropoelastin solution containing PF2 coated beads was then incubated at 40 °C. Coacervate directly reformed on the PF2 coated beads at (A) 80 s, (B) 85 s, (C) 90 s, and (D) 95 s after incubation. (E) After 30 min coacervate persisted on the bead while in solution the coacervate had settled.

Because less heat was absorbed by the system when PF2 was present, coacervation would naturally occur at lower temperatures. The positive entropy and enthalpy of this coacervating system puts tropoelastin in a small group of entropy-driven structure-forming processes. Previous studies on one member of this group, TMV, determined that, although the formation of a complex structure from free molecules in solution is a more ordered process and involves a decrease in entropy, this is over-balanced by an increase in entropy coming from the release of bulk water surrounding the protein (*38*, *39*). It is likely to occur in tropoelastin coacervation. The increase in entropy occurs as a result of the ordered water system being disrupted and released from the tropoelastin monomer (*14*). This over-balances the entropy contribution from the formation of a complex tropoelastin coacervate from free monomers in solution. We postulate that the smaller change in entropy values results as PF2 interacts with tropoelastin, prior to coacervation, and disrupts the ordered water around tropoelastin. Because the system is already disordered before coacervation takes place, a measure of the entropy or further disorder of the system during the process of coacervation would be lower than that of tropoelastin alone.

This result adds weight to the model in which the PF2 region of fibrillin-1 forms a major binding site on the microfibril to which tropoelastin localizes and coacervates around prior to cross-linking (*17*). To further test this model, we built an *in vitro* system in which a PF2-coated fixed surface was exposed to tropoelastin, the first of its kind. In solution, tropoelastin coacervate occurred as droplets of macromolecular aggregates of tropoelastin. This is the first time tropoelastin coacervation has been photographed in this way. These aggregates did not interact with a control surface. When the surface-bound PF2 was exposed to the tropoelastin, coacervate interaction took place as the aggregates coated the entire surface of the bead. After the reversible nature of the system was tested, a coacervate was again formed with the aggregates directly forming in contact with the beads.

This result fundamentally demonstrates the interaction of PF2 with tropoelastin. It shows that tropoelastin can directly form a coacervate around PF2 rather than migrating to PF2. It also demonstrates that tropoelastin coacervate can directly interact with a fixed surface as it does with the microfibril. Coacervate also persisted on this surface over a period of time. This *in vitro* model demonstrates the role of PF2 as one of the sites at which tropoelastin is initially deposited on the microfibril. This initiation step logically precedes the major coacervation that characterizes the expansion of elastin through coacervation and cross-linking (*29*). After initiation of elastogenesis as directed by microfibrils, expansion of the elastic fiber occurs by continued tropoelastin assembly. In summary, we now provide a more detailed model of the initial stages of elastogenesis in which the N-terminal domain of the tropoelastin monomer binds to the shoulder interbead region of the microfibril corresponding to the region encoded by PF2. Further tropoelastin interactions at other regions of the microfibril may also occur. Coacervation was thought to be solely a property of tropoelastin (*12*, *29*, *31*), but these

studies show that, when bound to PF2, tropoelastin coacervation is thermodynamically favorable as seen in the smaller change in enthalpy and entropy values. As coacervation continues, a mass increase occurs at this site as the coacervated tropoelastin is cross-linked to form elastin.

REFERENCES

1. Sakai, L. Y., Keene, D. R., and Engvall, E. (1986) Fibrillin, a new 350-kD glycoprotein, is a component of extracellular microfibrils, *J. Cell Biol. 103*, 2499−2509.
2. Kielty, C. M., Sherratt, M. J., and Shuttleworth, C. A. (2002) Elastic fibres, *J. Cell Sci. 115*, 2817−2828.
3. Gibson, M. A., Hatzinikolas, G., Kumaratilake, J. S., Sandberg, L. B., Nicholl, J. K., Sutherland, G. R., and Cleary, E. G. (1996) Further characterization of proteins associated with elastic fiber microfibrils including the molecular cloning of MAGP-2 (MP25), *J. Biol. Chem. 271*, 1096−1103.
4. Keene, D. R., Maddox, B. K., Kuo, H. J., Sakai, L. Y., and Glanville, R. W. (1991) Extraction of extendable beaded structures and their identification as fibrillin-containing extracellular matrix microfibrils, *J. Histochem. Cytochem. 39*, 441−449.
5. Henderson, M., Polewski, R., Fanning, J. C., and Gibson, M. A. (1996) Microfibril-associated glycoprotein-1 (MAGP-1) is specifically located on the beads of the beaded-filament structure for fibrillin-containing microfibrils as visualized by the rotary shadowing technique, *J. Histochem. Cytochem. 44*, 1389−1397.
6. Ross, R., Fialkow, R. J., and Altman, L. K. (1977) The morphogenesis of elastic fibers, *Adv. Exp. Med. Biol. 79*, 7−17.
7. Mecham, R., and Davis, E. C. (1994) (Yurchenco, P., Birk, D., and Mecham, R., Eds.) pp 281−314, Academic Press, Inc., San Diego, CA.
8. Vrhovski, B., and Weiss, A. (1998) Biochemistry of tropoelastin, *Eur. J. Biochem. 258*, 1−18.
9. Martin, S. L., Vrhovski, B., and Weiss, A. (1995) Total synthesis and expression in *Escherichia coli* of a gene encoding human tropoelastin, *Gene 154*, 159−166.
10. Indik, Z., Yeh, H., Ornstein-Goldstein, N., Kucich, U., Abrams, W., Rosenbloom, J. C., and Rosenbloom, J. (1989) Structure of the elastin gene and alternative splicing of elastin mRNA: Implications for human disease, *Am. J. Med. Genet. 34*, 81−90.
11. Indik, Z., Yoon, K., Morrow, S. D., Cicila, G., Rosenbloom, J., and Ornstein-Goldstein, N. (1987) Structure of the 3′ region of the human elastin gene: Great abundance of Alu repetitive sequences and few coding sequences, *Connect. Tissue Res. 16*, 197−211.
12. Vrhovski, B., Jensen, S., and Weiss, A. S. (1997) Coacervation characteristics of recombinant human tropoelastin, *Eur. J. Biochem. 250*, 92−98.
13. Urry, D. W. (1978) Molecular perspectives of vascular wall structure and disease: The elastic component, *Perspect. Biol. Med. 21*, 265−295.
14. Urry, D. W. (1988) Entropic elastic processes in protein mechanisms. I. Elastic structure due to an inverse temperature transition and elasticity due to internal chain dynamics, *J. Protein Chem. 7*, 1−34.
15. Reiser, K., McCormick, R. J., and Rucker, R. B. (1992) Enzymatic and nonenzymatic cross-linking of collagen and elastin, *FASEB J. 6*, 2439−2449.
16. Trask, T. M., Trask, B. C., Ritty, T. M., Abrams, W. R., Rosenbloom, J., and Mecham, R. P. (2000) Interaction of tropoelastin with the amino-terminal domains of fibrillin-1 and fibrillin-2 suggests a role for the fibrillins in elastic fiber assembly, *J. Biol. Chem. 275*, 24400−24406.
17. Rock, M. J., Cain, S. A., Freeman, L. J., Morgan, A., Mellody, K., Marson, A., Shuttleworth, C. A., Weiss, A. S., and Kielty, C. M. (2004) Molecular basis of elastic fiber formation: Critical interactions and a tropoelastin−fibrillin-1 cross-link, *J. Biol. Chem. 279*, 23748−23758.
18. Jensen, S. A., Reinhardt, D. P., Gibson, M. A., and Weiss, A. S. (2001) Protein interaction studies of MAGP-1 with tropoelastin and fibrillin-1, *J. Biol. Chem. 276*, 39661−39666.
19. Rodgers, U. R., and Weiss, A. (2004) Integrin avb3 binds a unique non-RGD site near the C-terminus of human tropoelastin, *Biochimie 86*, 173−178.
20. Laemmli, U. K. (1970) Cleavage of structural proteins during the assembly of the head of bacteriophage T4, *Nature 227*, 680−685.
21. Young, M. M., Tang, N., Hempel, J. C., Oshiro, C. M., Taylor, E. W., Kuntz, I. D., Gibson, B. W., and Dollinger, G. (2000) High throughput protein fold identification by using experimental constraints derived from intramolecular cross-links and mass spectrometry, *Proc. Natl. Acad. Sci. U.S.A. 97*, 5802−5806.
22. Schilling, B., Row, R. H., Gibson, B. W., Guo, X., and Young, M. M. (2003) MS2Assign, automated assignment and nomenclature of tandem mass spectra of chemically crosslinked peptides, *J. Am. Soc. Mass Spectrom. 14*, 834−850.
23. Lauffer, M. A. (1975) *Entropy-Driven Processes in Biology: Polymerisation of Tobacco Mosaic Virus Protein and Similar Reactions*, Chapman and Hall Ltd., London, U.K.
24. Smith, C. E., and Lauffer, M. A. (1967) Polymerization−depolymerization of tobacco mosaic virus protein. 8. Light-scattering studies, *Biochemistry 6*, 2457−2464.
25. Kaibara, K., Watanabe, T., and Miyakawa, K. (2000) Characterizations of critical processes in liquid−liquid-phase separation of the elastomeric protein−water system: Microscopic observations and light scattering measurements, *Biopolymers 53*, 369−379.
26. Sherratt, M. J., Holmes, D. F., Shuttleworth, C. A., and Kielty, C. M. (1997) Scanning transmission electron microscopy mass analysis of fibrillin-containing microfibrils from foetal elastic tissues, *Int. J. Biochem. Cell Biol. 29*, 1063−1070.
27. Kozel, B. A., Wachi, H., Davis, E. C., and Mecham, R. P. (2003) Domains in tropoelastin that mediate elastin deposition *in vitro* and *in vivo*, *J. Biol. Chem. 278*, 18491−18498.
28. Toonkool, P., Regan, D. G., Kuchel, P. W., Morris, M. B., and Weiss, A. S. (2001) Thermodynamic and hydrodynamic properties of human tropoelastin. Analytical ultracentrifuge and pulsed field-gradient spin−echo NMR studies, *J. Biol. Chem. 276*, 28042−28050.
29. Wise, S. G., Mithieux, S. M., Raftery, M. J., and Weiss, A. S. (2005) Specificity in the coacervation of tropoelastin: Solvent exposed lysines, *J. Struct. Biol. 149*, 273−281.
30. Wu, W. J., Vrhovski, B., and Weiss, A. S. (1999) Glycosaminoglycans mediate the coacervation of human tropoelastin through dominant charge interactions involving lysine side chains, *J. Biol. Chem. 274*, 21719−21724.
31. Muiznieks, L. D., Jensen, S. A., and Weiss, A. S. (2003) Structural changes and facilitated association of tropoelastin, *Arch. Biochem. Biophys. 410*, 317−323.
32. Kadler, K. E., Hulmes, D. J., Hojima, Y., and Prockop, D. J. (1990) Assembly of type I collagen fibrils *de novo* by the specific enzymic cleavage of pC collagen. The fibrils formed at about 37 °C are similar in diameter, roundness, and apparent flexibility to the collagen fibrils seen in connective tissue, *Ann. N.Y. Acad. Sci. 580*, 214−224.
33. Bellingham, C. M., Woodhouse, K. A., Robson, P., Rothstein, S. J., and Keeley, F. W. (2001) Self-aggregation characteristics of recombinantly expressed human elastin polypeptides, *Biochim. Biophys. Acta 1550*, 6−19.
34. Cox, B. A., Starcher, B. C., and Urry, D. W. (1973) Coacervation of α-elastin results in fiber formation, *Biochim. Biophys. Acta 317*, 209−213.
35. Jamieson, A. M., Downs, C. E., and Walton, A. G. (1972) Studies of elastin coacervation by quasielastic light scattering, *Biochim. Biophys. Acta 271*, 34−47.
36. Starcher, B. C., Saccomani, G., and Urry, D. W. (1973) Coacervation and ion-binding studies on aortic elastin, *Biochim. Biophys. Acta 310*, 481−486.
37. Toonkool, P., Jensen, S. A., Maxwell, A. L., and Weiss, A. S. (2001) Thermodynamic and hydrodynamic properties of human tropoelastin. Analytical ultracentrifuge and pulsed field-gradient spin−echo NMR studies, *J. Biol. Chem. 276*, 28042−28050.
38. Jaenicke, R., and Lauffer, M. A. (1969) Polymerization−depolymerization of tobacco mosaic virus protein. XII. Further studies on the role of water, *Biochemistry 8*, 3083−3092.
39. Stevens, C. L., and Lauffer, M. A. (1965) Polymerization−depolymerization of tobacco mosaic virus protein. IV. The role of water, *Biochemistry 10*, 31−37.
40. Clarke, A. W., and Weiss, A. S. (2004) Microfibril-associated glycoprotein-1 binding to tropoelastin: Multiple binding sites and the role of divalent cations, *Eur. J. Biochem. 271*, 3085−3090.

BI050530D